



ELSEVIER

journal homepage: [www.elsevier.com/locate/jmatprotec](http://www.elsevier.com/locate/jmatprotec)

# Analysis of the manufacturing process of beverage cans using aluminum alloy

Luis Fernando Folle\*, Sergio Eglan Silveira Netto, Lirio Schaeffer

Laboratory of Mechanical Transformation (LdTM), Faculty of Engineering, Federal University of Rio Grande do Sul, Brazil

## ARTICLE INFO

### Article history:

Received 27 June 2007

Received in revised form

31 October 2007

Accepted 20 November 2007

### Keywords:

Ironing

Beverage cans

Aluminum alloy

Forming limit curve

Friction coefficient

Strain-hardening exponent

## ABSTRACT

The parameters involved in the beverage cans manufacturing process have been analyzed by many authors. These parameters are used to determine the quality of the raw material before it is used to manufacture the cans. It is shown that the strain-hardening exponent together with the forming limit curve can predict whether the sheet metal will have a good drawability throughout its length. It is also shown how much others parameters such as angle of the ironing die, friction coefficient and clearance between punch and ironing die influence the ironing force and consequently the manufacturing process.

© 2007 Elsevier B.V. All rights reserved.

## 1. Introduction

Deep drawing and ironing are the most frequently used manufacturing processes to produce thin-walled cans. Due to their importance these processes are currently the subject of many studies (Rubio et al., 2006; Campion, 1980; Chang and Wang, 1997; Danckert, 2001; Penteado, 2002; Courbon, 2003; Gotoh et al., 2003; Hackworth and Henshaw, 2000; Jianjun, 1994; Kammerer et al., 1995; Kampus and Kuzman, 1995; Ragab and Orban, 2000; Yanran et al., 1995). Danckert (2001) shows that there is a thickness reduction rate in which the ironing process becomes unstable. This leads to a variation of thickness along the can in the circumferential direction. These problems are generally solved in the industry by trial and error, with changes in the material geometry.

Over the years, can thickness has diminished without reduction in mechanical resistance followed by added density

(Courbon, 2003). However, there are related problems such as the reject rate of defective cans during manufacturing, where for a given roll coil, there is a higher rate than for others. This, however, from the manufacturer's point of view is very difficult to predict, since there is no normalized method or equipment for this purpose.

## 2. Experimental procedure

The strain-hardening exponent, strain-hardening coefficient and plastic strain ratio were obtained using a tensile test to construct the stress curve versus true strain (DIN, 1991). Based on this curve, the flow curve is obtained that will supply the values of the strain-hardening exponent and strain-hardening coefficient. The plastic strain ratio ( $r$ ) is obtained with the same test, measuring the longitudinal and transverse dis-

\* Corresponding author.

E-mail address: [luis.folle@ufrgs.br](mailto:luis.folle@ufrgs.br) (L.F. Folle).

0924-0136/\$ – see front matter © 2007 Elsevier B.V. All rights reserved.

doi:10.1016/j.jmatprotec.2007.11.249

placements to obtain the respective longitudinal ( $\varphi_l$ ) and transversal ( $\varphi_b$ ) strains, which will be described below.

In the tensile test, the ratio between force ( $F$ ) and instantaneous area ( $A$ ) is flow stress  $k_f$ , Eq. (1):

$$k_f = \frac{F}{A} \quad (1)$$

To measure the longitudinal displacement, the INSTRON 2630-100 series Clip-on Extensometers sensor was used. This sensor has a precision of  $\pm 0.06\%$  FRO, which is connected to the test specimen for the purpose of obtaining strain  $\varepsilon$  of the material. With this value the true strain  $\varphi_l$ , can be found in the longitudinal direction which is used to construct the flow curve Eq. (2)

$$\varphi_l = \ln(1 + \varepsilon) \quad (2)$$

During the tensile test that determines the flow curve, the transversal displacement sensor INSTRON 2640-010 (static type) was used. This sensor has  $\pm 0.2\%$  FSD of error and was also used to connect in the same test specimen. According to standard SEW 1126 (1984) and the results obtained with this sensor, the strain ( $\varphi_b$ ) is reached. Through these two sensors the value of anisotropy  $r$  can be determined with Eq. (3).

$$r = \frac{\varphi_b}{\varphi_b + \varphi_l} \quad (3)$$

### 3. Results and analyses

#### 3.1. Strain-hardening exponent

The value of the strain-hardening exponent and of the strain-hardening coefficient is obtained based on standard SEW 1125 (1984). Strips were taken from the beginning, middle and end of each roll coil to make the test specimens. Experiments were performed to determine the strain-hardening exponent and the strain-hardening coefficient on the right, middle and left side of the sheet metal at  $0^\circ$ ,  $45^\circ$  and  $90^\circ$  compared to the direction of rolling. It was make three valid experiments per region. Using Eqs. (1) and (2), the flow curve is constructed and the adjusted Eq. (4) is the one that adjusts best to the curve mathematically.

$$k_f = C\varphi^n \quad (4)$$

where  $n$  is the strain-hardening exponent and  $C$  is the strain-hardening coefficient.

Tables 1 and 2 show these constants calculated for each of the rolling directions and the mean value which is used in Eq.

**Table 1 – Strain-hardening exponent**

$n$ at $0^\circ$	$0.210 \pm 0.005$
$n$ at $45^\circ$	$0.224 \pm 0.006$
$n$ at $90^\circ$	$0.227 \pm 0.006$
$n_{\text{mean}}$	$0.221 \pm 0.006$

Material: Roll coil 1.

**Table 2 – Strain-hardening coefficient (MPa)**

C at $0^\circ$	$359 \pm 6.9$
C at $45^\circ$	$365 \pm 6.9$
C at $90^\circ$	$381 \pm 7.1$
$C_{\text{mean}}$	$368 \pm 7.0$

Material: Roll coil 1.

(4). These results were made from a roll coil (called roll coil 1) that presented an excellent formation of the cans, throughout its length, and therefore no measurements were performed at the beginning and end.

After data on roll coil 1 were collected, new experiments were performed with samples collected from roll coils 2 and 3. Strips were extracted from these roll coils at the beginning, middle and end. With these strips tensile tests were performed to determine the strain-hardening exponent, Tables 3 and 4, and strain-hardening coefficient, Tables 5 and 6.

From the results in Tables 3 and 4 it is seen that there is a hardening gradient along the roll coil, since a decrease is observed in the direction of its end. This denotes that the formation of cans at the end of the roll coil is worse (center when the roll coil is rolled up), which may cause a greater number of defective samples. The strain-hardening coefficient values,

**Table 3 – Strain-hardening exponent**

Region of roll coil	Left	Middle	Right
Beginning	$0.101 \pm 0.003$	$0.190 \pm 0.005$	$0.137 \pm 0.004$
Middle	$0.095 \pm 0.005$	$0.098 \pm 0.002$	$0.101 \pm 0.003$
End	$0.097 \pm 0.003$	$0.086 \pm 0.014$	$0.079 \pm 0.001$

Material: Roll coil 2.

**Table 4 – Strain-hardening exponent**

Region of roll coil	Left	Middle	Right
Beginning	$0.171 \pm 0.005$	$0.172 \pm 0.001$	$0.136 \pm 0.010$
Middle	$0.102 \pm 0.003$	$0.097 \pm 0.005$	$0.092 \pm 0.003$
End	$0.077 \pm 0.004$	$0.083 \pm 0.002$	$0.070 \pm 0.003$

Material: Roll coil 3.

**Table 5 – Strain-hardening coefficient**

Region of roll coil	Left	Middle	Right
Beginning	$361 \pm 16$	$421 \pm 13$	$390 \pm 18$
Middle	$382 \pm 19$	$386 \pm 22$	$379 \pm 20$
End	$385 \pm 10$	$379 \pm 21$	$358 \pm 10$

Material: Roll coil 2.

**Table 6 – Strain-hardening coefficient**

Region of roll coil	Left	Middle	Right
Beginning	$375 \pm 28$	$382 \pm 25$	$379 \pm 26$
Middle	$470 \pm 14$	$429 \pm 25$	$389 \pm 22$
End	$378 \pm 20$	$381 \pm 10$	$377 \pm 15$

Material: Roll coil 3.

Table 7 – Anisotropy with 20% strain	
r at 0°	0.852 ± 0.026
r at 45°	0.914 ± 0.024
r at 90°	0.892 ± 0.005
r	0.893 ± 0.019
Material: Roll coil 1.	

Tables 2, 5 and 6, did not present significant variations, therefore the study did not focus on this.

### 3.2. Plastic strain ratio

Using the longitudinal and transversal sensors specifically to measure displacement in the direction of length and width, strains were measured in the three rolling directions, where a weighted mean is shown. Applying Eq. (3) to a 20% strain, the anisotropy of the material is defined as seen in Table 7.

### 3.3. Forming limit curve

For the Nakajima test it was used a hemispheric-type punch with a 50 mm radius for the experiment. In order to reduce friction as much as possible, a 7-mm-thick of polyurethane cushion was used according to work made by Silveira Netto et al. (2003) and reference ISO (1997). The polyurethane is used like a lubricant and prevents the contact between the punch and the sheet metal in order to get better the strain distribution in the sheet metal.

Fig. 1 shows the measurements performed, after the experiments, for test specimens taken from the beginning, middle and end of the roll coil. Under these points, a polynomial is created which is the FLC. The curve for the beginning and middle of the roll coil is the same.

Analyzing these results it is seen that the continuous curve for the end has a lower limit than the others regions, showing that at the end of the roll coil the drawability of the material is not a good as at the beginning or at the end.

## 4. Influence of various parameters on the ironing force

The following analyses are from of the equation that calculates the force in the ironing process. The influence of the

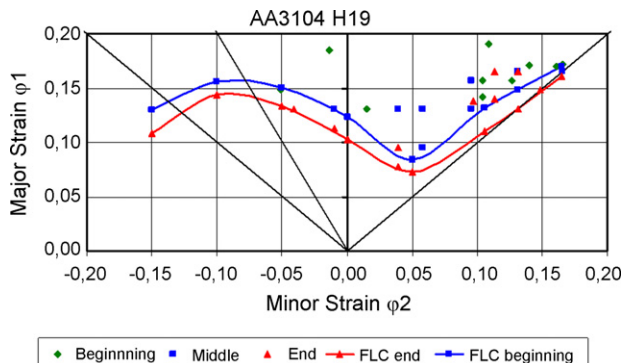


Fig. 1 – Forming limit curve. Material: Roll coil 3.

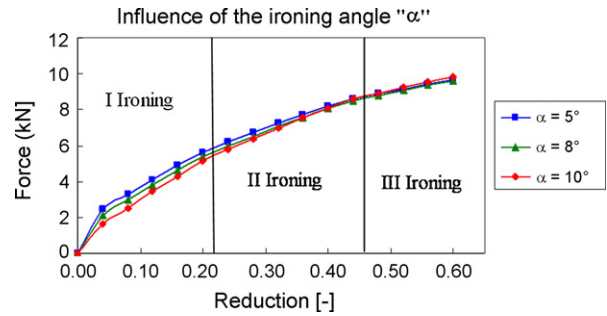


Fig. 2 – Influence of the ironing die angle on force.

parameters die angle, friction coefficient, strain-hardening exponent, clearance between the punch and the ironing die and limit of drawing are separately varied while the other parameters stay constant.

The ironing force is calculated by Eq. (5) described by Schaeffer (1999).

$$F = kf_m A_1 \varphi_A \left( 1 + \frac{\mu}{\alpha} + \frac{2\alpha}{3\varphi_A} \right) \tag{5}$$

where  $kf_m$  is the mean between radial stress before and after the corresponding ironing stage,  $A_1$  is the cross-sectional area of the can after ironing,  $\varphi_A$  is the main strain involved,  $\alpha$  is the ironing die angle and  $\mu$  is the friction coefficient.

For the all calculation, except for the influence on the force, the coefficient of friction was adjusted to 0.02 according of the studied made by Chang and Wang (1997).

### 4.1. Influence of the ironing die angle on the force

On entering the first ironing die, the material thickness has not yet been reduced, and therefore does not show any strain. As the material passes through the ironing die, there is a sudden rise in the ironing force up to the value indicated in Fig. 2, where force is plotted in relation to the reduction of thickness. In subsequent ironings force continues to increase up to the value of maximum thickness reduction.

Fig. 2 shows the influence of the ironing die angle on the ironing force compared to the reduction of thickness. A small variation in force can be seen for a considerable increase in the ironing die angle, where this variation reaches almost zero at the last ironing.

### 4.2. Influence of the friction coefficient on force

As can be seen in Fig. 3, the friction coefficient between the material and the ironing die significantly influences the ironing force, and at every stage of ironing this difference increases further. This shows that the greater the force applied to the material, the greater the influence of friction on the process. The limit of drawing was calculated and shown in Table 8 for each stage of ironing with different friction coefficients arbitrated, where it can be perceived that it increases as the ironing stages advance. It can also be seen that the limit of drawing for the third ironing and friction coefficient of 0.10 is greater than 0.866, which, according to literature Rubio et al. (2006),

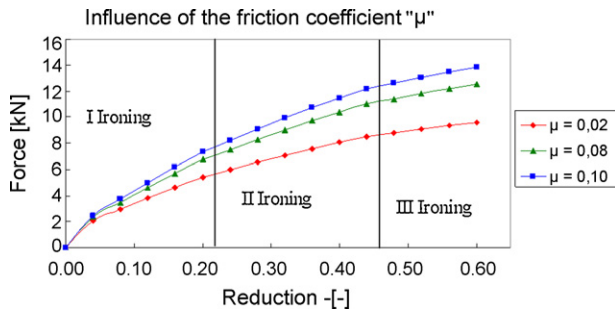


Fig. 3 – Influence of the friction coefficient on force.

Table 8 – Limit of drawing relating to the friction coefficient

Friction coefficient	1st ironing	2nd ironing	3rd ironing
0.02	0.32	0.42	0.60
0.08	0.43	0.56	0.83
0.10	0.47	0.62	0.91

can cause micro fissures inside the material, diminishing its quality.

4.3. Influence of the strain-hardening exponent on force

The strain-hardening exponent is a very important parameter for the sheet metal forming process. The higher its value, the greater will be the resistance of the material and the greater the absorption of strain, but the more force will be needed to press and ironing the material. This is shown in Fig. 4 where can be seen that the greater the strain-hardening exponent, the more force will be needed for ironing.

4.4. Influence of the clearance between the punch and the ironing die on force

In Fig. 5, it is shown that for a greater clearance there is a reduction in the ironing force and for a smaller clearance there is increased force, where the greatest influence of the clearance is in the third ironing. This shows that if there is a misalignment between the punch and the ironing die, there will be a

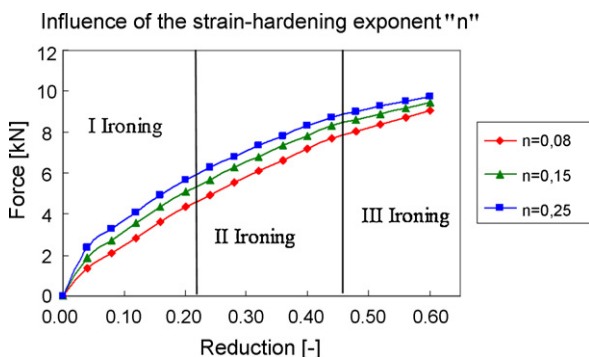


Fig. 4 – Influence of the strain-hardening exponent on force.

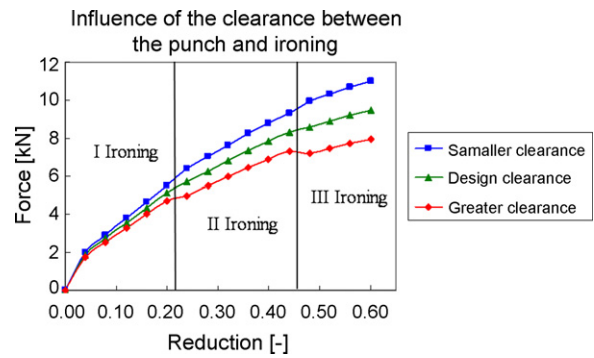


Fig. 5 – Influence of the clearance between the punch and ironing die on force.

significant imbalance in force and consequent excessive wear of the punch and ironing die.

4.5. Influence of the strain-hardening exponent on the limit of drawing

Maximum reduction (limit of drawing) is given by Eq. (6). The maximum degree admissible (a) found by Rubio et al. (2006) is 0.866. Values above 0.866 can cause the beginning of micro-cracks in the material and indicate that the process is not feasible.

$$a = \frac{\sigma_1}{kf_1} \leq 0.866 \tag{6}$$

where  $\sigma_1$  is axial stress (see Fig. 6) which is the ratio of ironing force  $F$  and the area at the end of the ironing die  $A_1$  see Eq. (7) and  $kf_1$  is the radial stress which is the stress corresponding to the deformation after the present ironing stage. Ironing force is given by Eq. (5).

$$\sigma_1 = \frac{F}{A_1} \tag{7}$$

Using the data obtained, a diagram is obtained between the limit of drawing and the final thickness of the can, varying the strain-hardening exponent. Fig. 7 shows that:

- to obtain a final can thickness (3° ironing) of 0.098 mm (design condition) there is 0.6 or 60% of limit of drawing if the strain-hardening exponent is 0.22;

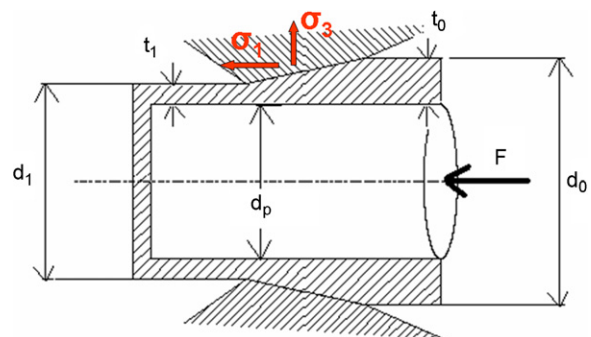
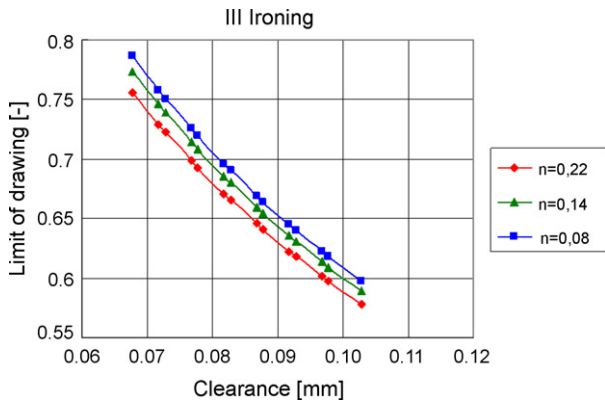


Fig. 6 – Schematic of each stage of ironing (font: Altan et al. (1999)).



**Fig. 7 – Relationship of limit of drawing, hardening and can thickness.**

- if the strain-hardening exponent diminishes, there is an increased in the limit of drawing of the material, maintaining the design condition;
- if there is a variation in the final thickness of the can wall, the figure shows which would be the limit of drawing obtained for known strain-hardening exponent.

Fig. 7 relates mechanical and metallurgical properties and tool design.

**4.6. Influence of various parameters considered together**

The influence of the previously analyzed parameters on the ironing force is shown in Fig. 8 where they are considered together (in the same graph). As can be seen the largest influence in the ironing force is the friction coefficient. The clearance between punch and the ironing die also had a high influence, however smaller than the friction coefficient. This shows the importance of a correct lubrication between the tools and the sheet metal. The strain-hardening exponent and

die angle did not have an influence on the force that could be relevant.

**5. Conclusions**

The manufacturing process for aluminum beverage cans is already technologically very advanced, and therefore it is useful to have the utmost information possible on material and tooling, in order to optimize it.

The strain-hardening exponent is seen to vary along the roll coil, diminishing towards the end. This causes more production scrap, and shows the importance of this factor in the quality of the cans produced. Thus, it is possible to perform quality control by means of tensile tests in the roll coils received by the factory, by monitoring the strain-hardening exponent and thus having a guarantee that the raw material is of good quality and will generate cans without any defects.

Anisotropy of the material proved very satisfactory, since it was very close to the unit, i.e., almost isotropic (Table 7).

The calculations of tooling force and analysis show that the material is not being submitted to the utmost requirements, and therefore a graph is constructed (Fig. 7), which shows that if the manufacturing wants to reduce the final can thickness, there is a possibility to explore more of the material without cause defects. These curves map the possibilities that, together with the FLC (Fig. 1), can be combined and used as a possibility by the can manufacturer.

Another important aspect observed was the influence of the following parameters: ironing die angle, friction coefficient, strain-hardening exponent and clearance between the punch and ironing die on ironing force. It was seen that, as was to be expected, the friction coefficient and the clearance between punch and ironing die have great influence on the manufacturing process. The ironing die angle, however, did not prove to be essential to the process, and did not influence force very much. The strain-hardening exponent had a similar influence on each ironing, and, as was to be expected, the higher its value, the more resistant is the material and the greater the force needed to strain it.

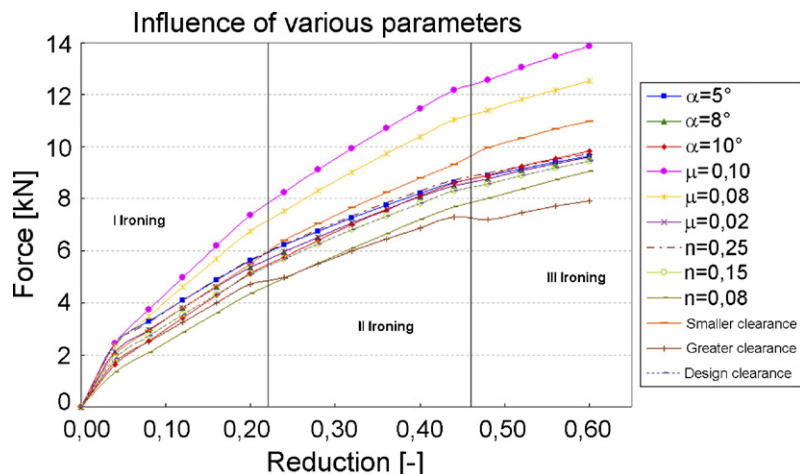


**Fig. 8 – Influence of various parameters on force.**

## Acknowledgements

The authors thank CNPq for funding the scholarships. We also thank REXAM BEVERAGE CANS AMERICAS for supplying the raw material.

## REFERENCES

- Altan, T., Oh, S., Gegel, H.L., 1999. *Conformação de metais - fundamentos e aplicações*. EESC-USP, São Carlos/SP. 350 pp.
- Campion, D., 1980a. Deep drawing and ironing—theory and practice. *Sheet Met. Ind.*, 111–119.
- Campion, D., 1980b. Deep drawing and ironing—theory and practice: 2. *Sheet Met. Ind.*, 330–341.
- Campion, D., 1980c. Deep drawing and ironing—theory and practice: Part 3. *Sheet Met. Ind.*, 563–566.
- Campion, D., 1980d. Deep drawing and ironing—theory and practice: Part 4 Practical considerations. *Sheet Met. Ind.*, 830–836.
- Chang, D.F., Wang, J.E., 1997. Influence of process parameters on the ironing of deep-drawn cups. *J. Manuf. Sci. Eng.* 119, 699–705.
- Courbon, J., 2003. Damage evolution in a compressive forming process: ironing of beverage cans. *Scr. Mater.* 48, 1519–1524.
- Danckert, J., 2001. Ironing of thin walled cans. *Ann. CIRP* 50, 165–168.
- Deutsches Institut Für Normung, 1991. *Din EN 10002: Tensile testing of metallic materials*. Berlin.
- Gotoh, M., Kim, Y.S., Yamashita, M., 2003. A fundamental study of can forming by the stretch-drawing process. *J. Mater. Process. Technol.* 138, 545–550.
- Hackworth, M.R., Henshaw, J.M., 2000. A pressure vessel fracture mechanics study of the aluminium beverage can. *Eng. Frac. Mech.* 65, 525–539.
- International Organization for Standard, 1997. *ISO 12004: Metallic Materials—Guidelines for the Determination of Forming-Limit Diagram*. Suisse.
- Jianjun, W., 1994. *The Calculation of Ironing Force*. Elsevier Science B.V, pp. 462–467.
- Kammerer, M., Pöhlandt, K., Tekkaya, A.E., 1995. Non-conventional extrusion of less-common materials. *J. Mater. Process. Technol.* 49, 345–354.
- Kampus, Z., Kuzman, K., 1995. Analysis of the factors influencing the geometrical shape of workpieces produced by ironing. *J. Mater. Process. Technol.* 49, 313–332.
- Penteado, E., 2002. *Fabricação de Latas de Alumínio pelo Processo de Drawing Ironing*. In: V Conferência Nacional de Conformação de Chapas. [Anais]. Gráfica e Editora Brasil, Gramado, RS, pp. 183–208.
- Ragab, M.S., Orban, H.Z., 2000. Effect of ironing on the residual stresses in deep drawn cups. *J. Mater. Process. Technol.* 99, 54–61.
- Rubio, E.M., Gonzálves, C., Marcos, M., Sebastián, M.A., 2006. Energetic analysis of tube drawing processes with fixed plug by upper bound method. *J. Process. Technol.* 177, 175–178.
- Schaeffer, L., 1999. *Conformação Mecânica*. Imprensa Livre, Porto Alegre. 167 pp.
- Stahl-Eisen-Werkstoffprüfblatt, 1984. SEW1125: Ermittlung des Verfestigungsexponenten (n-Wert) von Feinblech aus dem Zugversuch. Düsseldorf.
- Stahl-Eisen-Werkstoffprüfblatt, 1984. SEW1126: Ermittlung der senkrechten Anisotropie (r-Wert) von Feinblech aus dem Zugversuch. Düsseldorf.
- Silveira Netto, S.E., Malveira, N.N., Crivellaro, R.S., Borsoi, C.A., Schaeffer, L., 2003. Determinação da curva limite de conformação para alumínio aeronáutico 6061-O. In: *Congresso Brasileiro de Engenharia de Fabricação (2.: 2003: Uberlândia)*. [Anais]. Bit House Brasil, Uberlândia, MG (COF03-0017.pdf (260.8 KB)).
- Yanran, Z., Wang, Z.R., Weimin, C., 1995. Numerical simulations for extrusion and ironing and die-angle optimisation. *J. Mater. Process. Technol.* 55, 48–52.